

Bayesian Non Local Means-Based Speckle filtering

Pierrick Coupé, Pierre Hellier, Charles Kervrann, Christian Barillot

► **To cite this version:**

Pierrick Coupé, Pierre Hellier, Charles Kervrann, Christian Barillot. Bayesian Non Local Means-Based Speckle filtering. IEEE International Symposium on Biomedical Imaging: From Nano to Macro, May 2008, Paris, France. 2008. <inria-00283477>

HAL Id: inria-00283477

<https://hal.inria.fr/inria-00283477>

Submitted on 30 May 2008

HAL is a multi-disciplinary open access archive for the deposit and dissemination of scientific research documents, whether they are published or not. The documents may come from teaching and research institutions in France or abroad, or from public or private research centers.

L'archive ouverte pluridisciplinaire **HAL**, est destinée au dépôt et à la diffusion de documents scientifiques de niveau recherche, publiés ou non, émanant des établissements d'enseignement et de recherche français ou étrangers, des laboratoires publics ou privés.

BAYESIAN NON LOCAL MEANS-BASED SPECKLE FILTERING

Pierrick Coupé^{1,2,3}, Pierre Hellier^{1,2,3}, Charles Kervrann^{4,5} and Christian Barillot^{1,2,3}

¹ University of Rennes I, CNRS UMR 6074, IRISA, Rennes, France

² INRIA, VisAGeS Project, IRISA, Rennes, France

³ INSERM, U746 Unit, IRISA, Rennes, France

⁴ INRIA, VISTA Project, IRISA, Rennes, France

⁵ INRA-MIA, Domaine de Vilvert, 78352 Jouy en Josas, France

ABSTRACT

In ultrasound (US) imaging, denoising is intended to improve quantitative image analysis techniques. In this paper, a new version of the Non Local (NL) Means filter adapted for US images is proposed. Originally developed for Gaussian noise removal, a Bayesian framework is used to adapt the NL means filter for speckle noise. Experiments were carried out on synthetic data sets with different speckle simulations. Results show that our NL means-based speckle filter outperforms the classical implementation of the NL means filter, as well as two other speckle adapted denoising methods (SRAD and SBF filters).

Index Terms— Image restoration, Image enhancement, Acoustics, Acoustic applications

1. INTRODUCTION AND RELATED WORK

Denoising is a particularly challenging problem in ultrasound (US) imaging since the signal-to-noise ratio is low. Contrary to the Gaussian noise model assumed in usual denoising methods, US imaging requires specific filters due to the statistical nature of the speckle. Speckle in US images is useful for the radiologist since this signal contains information about the density and the size of scatters. Nonetheless, the speckle is often considered as noise by the image processing community, because its presence spoils medical image analysis procedures. For this reason, denoising filters have been developed. The well known adaptive filters, such as Lee's filter [1], Frost's filter [2], and Kuan's filter [3], are based on the hypothesis that speckle noise is essentially a multiplicative noise. More recently, the Adaptive Speckle Reduction filter (ASR) [4] uses local statistics of the image to estimate the areas of the image to be processed. The classical formulations of Anisotropic Diffusion filter (AD) [5] and Total Variation minimization scheme (TV) [6] have been adapted for US imaging as Speckle Reducing Anisotropic Diffusion (SRAD) filter [7] or the Non-Linear Coherent Diffusion (NCD) filter [8]. The classical wavelet thresholding postulates that the logarithm compression of the US images transforms speckle noise

into additive Gaussian noise. In order to overcome this assumption, Pizurica *et al.* [9] proposed a method without prior model on the noise and signal statistics. Recently, a stochastic approach to ultrasound despeckling (SBF) has been developed [10]. This method removes the local extrema, considered as outliers, by local averaging.

In this paper, we introduce a new restoration scheme in the context of US imaging : a Non Local (NL) Means-based Speckle Filter. The NL means filter was earlier introduced by Buades *et al.* [11] for Gaussian noise reduction. The main contribution of this paper is the adaptation of this filter to US noise model based on the Bayesian formulation of the NL means filter presented in [12] and the US noise model proposed in [13]. A comparison of our method with SRAD [7], SBF [10] and the classical NL means filters [11] is presented for different levels of noise and speckle simulations.

2. THE NL MEANS-BASED SPECKLE FILTER

2.1. The Non Local Means Filter

In the classical formulation of the NL means filter [11], the restored intensity $NL(u)(x_i)$ of the pixel x_i , is a weighted average of the pixels intensities $u(x_i)$ in the “search volume” V_i . Let us denote :

$$NL(u)(x_i) = \sum_{x_j \in V_i} w(x_i, x_j) u(x_j) \quad (1)$$

where $w(x_i, x_j)$ is the weight assigned to intensity value $u(x_j)$ for restoration of pixel x_i . For each pixel x_j in V_i , the L_2 -norm $\|\cdot\|_2^2$ is computed between $u(N_j)$ (the neighborhood of x_j) and $u(N_i)$ (the neighborhood of x_i). Then, these distances are weighted by the weighting function defined as follows :

$$w(x_i, x_j) = \frac{1}{Z_i} e^{-\frac{\|u(N_i) - u(N_j)\|_2^2}{h^2}} \quad (2)$$

where Z_i is the normalization constant ensuring that $\sum_{x_j \in V_i} w(x_i, x_j) = 1$, and h acts as a smoothing parameter. This filter produces high quality denoising but it is computationally expensive.

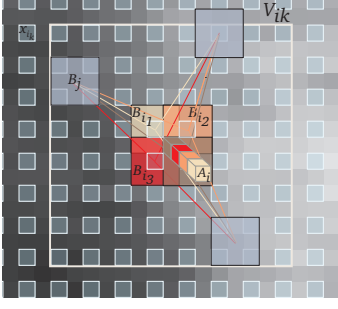


Fig. 1. Blockwise NL means filter.

2.2. Blockwise Approach

To reduce the computational complexity of the algorithm, we introduce a blockwise approach. In our blockwise NL-means filter, a weighted average of patches is performed instead of weighted average of pixel intensities (cf Fig. 1). The blockwise approach consists in a) dividing the volume into blocks with overlapping supports ; b) performing NL means-like restoration of these blocks ; c) restoring the pixels values based on the restored intensities of the blocks they belong to :

a) A partition of the image Ω into overlapping blocks B_{i_k} of size $P = (2\alpha + 1)^d$ is performed (d is the dimensionality of the image : 2 or 3), such as $\Omega = \bigcup_k B_{i_k}$, under the constraint that the intersections between the blocks B_{i_k} are non-empty (i.e. $2\alpha \geq n$). These blocks are centered on pixels x_{i_k} which constitute a subset of Ω . The x_{i_k} are equally distributed at positions $i_k = (k_1 n, k_2 n, k_3 n)$, $(k_1, k_2, k_3) \in \mathbb{N}^d$ where n represents the distance between the centers of B_{i_k} .

b) the restoration of a block B_{i_k} is based on a NL means scheme defined as follows :

$$\mathbf{NL}(u)(B_{i_k}) = \sum_{B_j \in V_{i_k}} w(x_{i_k}, x_j) \mathbf{u}(B_j) \quad (3)$$

with

$$w(x_{i_k}, x_j) = \frac{1}{Z_{i_k}} e^{-\frac{\|\mathbf{u}(B_{i_k}) - \mathbf{u}(B_j)\|_2^2}{h^2}} \quad (4)$$

where $\mathbf{u}(B_i) = (u^{(1)}(B_i), \dots, u^{(P)}(B_i))^T$ is an image patch containing the intensities of the block B_i , Z_{i_k} is a normalization constant ensuring that $\sum_j w(x_{i_k}, x_j) = 1$ and

$$\|\mathbf{u}(B_i) - \mathbf{u}(B_j)\|_2^2 = \sum_{p=1}^P (u^{(p)}(B_i) - u^{(p)}(B_j))^2. \quad (5)$$

c) For a pixel x_i included in several blocks B_{i_k} , several estimations of the same pixel x_i from different $\mathbf{NL}(u)(B_{i_k})$ are computed and stored in a vector \mathbf{A}_i (cf Fig. 1). The final restored intensity of pixel x_i is then defined as :

$$NL(u)(x_i) = \frac{1}{|\mathbf{A}_i|} \sum_{l \in \mathbf{A}_i} \mathbf{A}_i(l). \quad (6)$$

This approach allows to significantly reduce the complexity of the algorithm. For instance, if we set $n = 2$, the complexity is divided by a factor 4 in 2D and 8 in 3D.

2.3. Bayesian Formulation

Based on the recent Bayesian interpretation of the NL means filter [12], the blockwise NL means can be written as :

$$\mathbf{NL}(u)(B_{i_k}) = \frac{\frac{1}{|V_{i_k}|} \sum_{j=1}^{|V_{i_k}|} p(\mathbf{u}(B_{i_k}) | \mathbf{u}(B_j)) p(\mathbf{u}(B_j)) \mathbf{u}(B_j)}{\frac{1}{|V_{i_k}|} \sum_{j=1}^{|V_{i_k}|} p(\mathbf{u}(B_{i_k}) | \mathbf{u}(B_j)) p(\mathbf{u}(B_j))} \quad (7)$$

where $p(\mathbf{u}(B_{i_k}) | \mathbf{u}(B_j))$ and $p(\mathbf{u}(B_j))$ respectively denote the distribution of $\mathbf{u}(B_{i_k}) | \mathbf{u}(B_j)$ and the prior distribution of patches (assumed to be uniform in what follows). This new formulation has the advantage to allow the adaptation of the NL means filter to the underlying noise distribution.

2.4. Noise Model in Log-compressed US Images

Realistic modeling of noise distribution of US images is difficult to establish for various reasons : (a) local correlation due to periodic arrangements of scatterers [7], (b) envelope detection and logarithm amplification of radio-frequency signals performed on the displayed image [8], (c) additive Gaussian noise due to sensors [8] and (d) additive Gaussian noise related to A/N acquisition cards, tend to invalidate the Rayleigh model of RF signal for US Log-compressed images. In the wavelet denoising domain [8], the logarithmic operation is assumed to transform speckle noise into additive Gaussian noise. Recent studies on US images show that the distribution of noise is closer to the Gamma distribution [14] or Fisher-Tippett distribution [15]. Another way to deal with the problem of noise modeling in US images is to use a more general image model defined as $u(x) = v(x) + v^\gamma(x)\eta(x)$ where $v(x)$ is the original image, $u(x)$ is the observed image, $\eta(x)$ is a zero-mean Gaussian noise of variance σ^2 and $\gamma = 0.5$. This model was first introduced for ultrasound image denoising by Loupas *et al.* in [13] and then has been often used [16]. Contrary to the Gaussian noise model, this noise model is image-dependent and takes into account that speckle noise amplitude is larger in regions of high intensities [14, 16].

2.5. A New Statistical Distance for Patch Comparison : the Pearson Distance

Based on the Bayesian formulation (see Eq. (7)), we introduce a new scheme to compute the distance between image patches based on the noise model : $u(x) = v(x) + \sqrt{v(x)}\eta(x)$, $\eta(x) \sim \mathcal{N}(0, \sigma^2)$. We have $u(x) | v(x) \sim \mathcal{N}(v(x), v(x)\sigma^2)$, i.e. $p(u(x) | v(x)) \propto \exp -\frac{(u(x) - v(x))^2}{2v(x)\sigma^2}$. The likelihood can be factorized for a block as :

$$p(\mathbf{u}(B_i) | \mathbf{u}(B_j)) = \prod_{p=1}^P p(u^{(p)}(x_i) | u^{(p)}(x_j)) \quad (8)$$

$$\propto \exp - \sum_{p=1}^P \frac{(u^{(p)}(x_i) - u^{(p)}(x_j))^2}{2u^{(p)}(x_j)\sigma^2}. \quad (9)$$

The Pearson distance is then substituted to the usual L_2 -norm (see Eq. (5)).

$$d_P(\mathbf{u}(B_i), \mathbf{u}(B_j)) = \sum_{p=1}^P \frac{(u^{(p)}(B_i) - u^{(p)}(B_j))^2}{u^{(p)}(B_j)}. \quad (10)$$

This new distance allows to smooth bright areas more than dark areas, and then to be more adapted to speckle statistics. As in [12, 17], pixel selection in the search area is applied to speed up the filter and to better preserving contrast.

$$w(x_{i_k}, x_j) = \begin{cases} \frac{1}{Z_{i_k}} e^{-\frac{d_P(\mathbf{u}(B_{i_k}), \mathbf{u}(B_j))}{h^2}} & \text{if } \mu_1 < \frac{\mathbf{u}(B_{i_k})}{\mathbf{u}(B_j)} < \frac{1}{\mu_1} \\ 0 & \text{otherwise.} \end{cases} \quad (11)$$

μ_1 is an hyper-parameter controlling the pixel selection whose the value will be fixed for all the experiments. Compared to the classical formulation, our Optimized Bayesian Non Local Means filter (OBNLM) includes the Pearson distance for weight computation, the pixel selection and the blockwise implementation.

3. EXPERIMENTS

To evaluate the performances of our filter, different experiments were carried out on synthetic images with two different models of speckle. The speckle models used during experiments were different to the model used in our method in order to perform a fair comparison. In the first experiment, a synthetic image available in Matlab was corrupted with different levels of noise. The applied simulation of the speckle was the Matlab speckle model : $u(x_i) = v(x_i) + v(x_i)\nu(x_i)$, $\nu(x_i) \sim \mathcal{N}(0, \sigma^2)$. Three levels of noise were tested with $\sigma = [0.2, 0.4, 0.8]$. To quantify the quality of the denoising obtained with the compared methods, the Signal to Noise Ratio (SNR) was computed between the ‘‘ground truth’’ and the denoised images.

$$SNR = 10 \log_{10} \frac{\sum_{x_i \in \Omega} (v(x_i)^2 + \tilde{v}(x_i)^2)}{\sum_{x_i \in \Omega} (v(x_i) - \tilde{v}(x_i))^2} \quad (12)$$

where $v(x_i)$ is the true value of the pixel and $\tilde{v}(x_i)$ the restored intensity of the pixel. For each method, at each noise level, the optimal filter parameters were searched within a large range. Tab. 1 shows the SNR obtained during the comparison. For all levels of noise, our OBNLM filter significantly obtained the best SNR. Fig. 2 shows the denoising results for $\sigma = 0.4$. In the second experiment, we used the validation framework proposed in [10]. In order to evaluate the compared denoising filters with a more realistic speckle simulation, the physical modeling of speckle presented in [18] was applied on a synthetic phantom (Field II). The denoising performance of each filter is given by the ultrasound despeckling assessment index (\tilde{Q}) as defined in [10]. According to [10], a higher \tilde{Q} indicates a better denoising. Fig. 3 presents the denoising results obtained for the compared methods and the corresponding \tilde{Q} indexes. Similar values than those presented in [10] were found for SRAD and SBF filters. Compared

to the classical NL means filter, our method significantly improves the \tilde{Q} index (around 40%). In this evaluation framework, our OBNLM filter obtained the highest \tilde{Q} index. Finally, examples of denoising obtained on real data acquired during neurosurgical procedure is given in Fig. 4. Our blockwise implementation processes an image of 390×500 pixels in 6s on a Pentium M 2GHz. Visually, our filter efficiently removed the speckle while enhancing the edges and preserving the image structures. The SRAD and SBF filters removed speckle but produced artifacts (local constant areas and artificial structures). These artifacts are also visible in the experiments on synthetic data sets, especially in Fig. 3.

SNR			
Filter	$\sigma = 0.2$	$\sigma = 0.4$	$\sigma = 0.8$
Noisy phantom	39.32	25.96	14.11
SBF [10]	49.61	43.86	38.04
SRAD [7]	57.17	44.07	33.29
NLM [11]	62.15	47.92	38.72
OBNLM	64.13	53.12	42.13

Table 1. Quantitative results obtained with the compared filters for the 2D phantom study. Our OBNLM filter obtained the highest SNR for all noise levels.

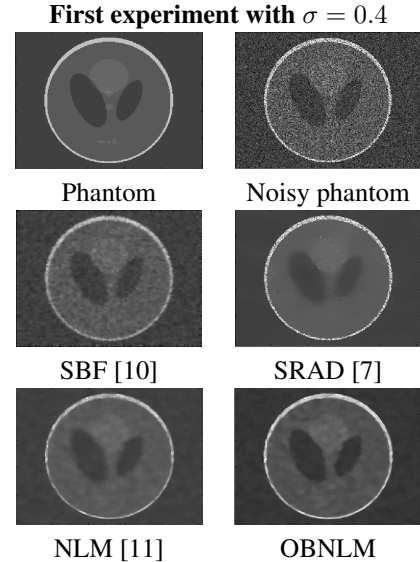


Fig. 2. Denoised images obtained by the compared filters in the first experiment.

4. CONCLUSION

In this paper, we proposed a Non Local (NL) means-based filter for US images by introducing the Pearson distance as a relevant measure for patch comparison. Evaluations were performed on synthetic data with different noise levels and different speckle simulations. Experiments showed that the proposed filter outperforms the classical implementation of the NL means filter as well as the SRAD and the SBF filters.

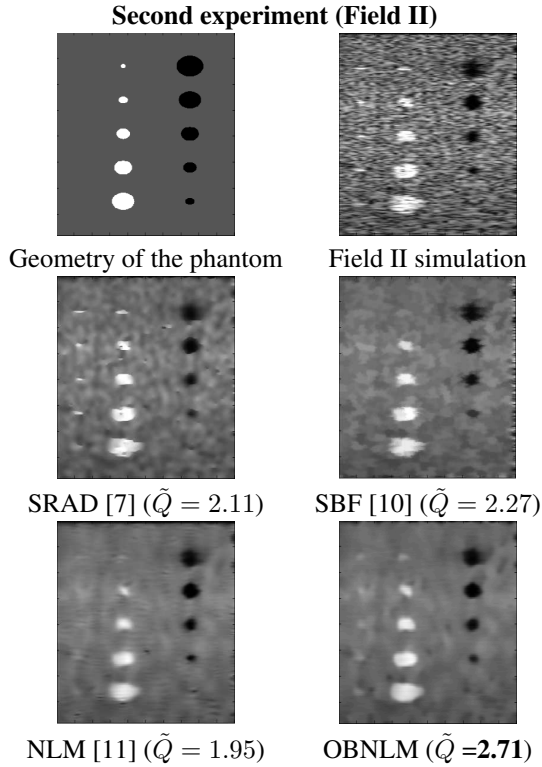


Fig. 3. Denoised images obtained by the compared filters and the corresponding \tilde{Q} index. Our filter obtained the highest \tilde{Q} index.

These results show that image-redundancy assumption required for NL means filter holds for ultrasound imaging. Further work will pursue on automatic tuning of filter parameters of our Optimized Bayesian NL means (OBNLM) filter. Finally, the impact of our method on post-processing tasks such as segmentation or registration will have to be studied.

5. REFERENCES

- [1] J. S. Lee, "Digital image enhancement and noise filtering by use of local statistics," *IEEE PAMI*, vol. 2, pp. 165–168, 1980.
- [2] V.S. Frost et al., "A model for radar images and its application to adaptive digital filtering of multiplicative noise," *IEEE PAMI*, vol. 2, pp. 157–65, 1982.
- [3] D.T Kuan et al., "Adaptive noise smoothing filter for images with signal-dependent noise," *IEEE PAMI*, vol. 7, no. 2, pp. 165–177, 1985.
- [4] A. Lopes et al., "Adaptive speckle filters and scene heterogeneity," *IEEE Trans. geosci. remote sensing*, vol. 28, pp. 992–1000, 1990.
- [5] P. Perona and J. Malik, "Scale-space and edge detection using anisotropic diffusion," *IEEE PAMI*, vol. 12, no. 7, pp. 629–639, 1990.
- [6] L.I. Rudin et al., "Nonlinear total variation based noise removal algorithms," *Physica D*, vol. 60, pp. 259–268, 1992.
- [7] Y. Yu and S. T. Acton, "Speckle reducing anisotropic diffusion," *IEEE TIP*, vol. 11, no. 11, pp. 1260–1270, 2002.
- [8] K. Z. Abd-Elmoniem et al., "Real-time speckle reduction and coherence enhancement in ultrasound imaging via nonlinear anisotropic diffusion," *IEEE TBE*, vol. 49, no. 9, pp. 997–1014, 2002.

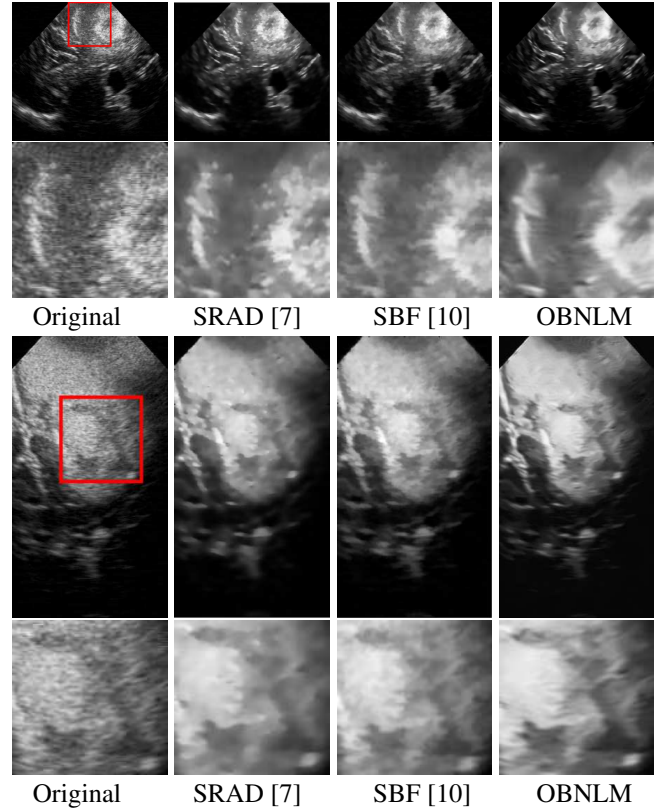


Fig. 4. Results obtained with SRAD, SBF and the proposed filters on real intraoperative brain images with zooms. Our filter efficiently removes the speckle while enhancing the edges and preserving the image structures.

- [9] A. Pizurica et al., "A review of wavelet denoising in mri and ultrasound brain imaging," *Current Medical Imaging Reviews*, vol. 2, no. 2, pp. 247–260, 2006.
- [10] P. C. Tay et al., "A stochastic approach to ultrasound despeckling," in *ISBI'06*, 2006, pp. 221–224.
- [11] A. Buades et al., "A review of image denoising algorithms, with a new one," *Multiscale Modeling & Simulation*, vol. 4, no. 2, pp. 490–530, 2005.
- [12] C. Kervrann et al., "Bayesian non-local means filter, image redundancy and adaptive dictionaries for noise removal," in *SSVM' 07*, 2007, pp. 520–532.
- [13] T. Loupas et al., "An adaptive weighted median filter for speckle suppression in medical ultrasound image," *IEEE T. Circ. Syst.*, vol. 36, pp. 129–135, 1989.
- [14] Z. Tao et al., "Evaluation of four probability distribution models for speckle in clinical cardiac ultrasound images," *IEEE TMI*, vol. 25, no. 11, pp. 1483–1491, 2006.
- [15] G. Slabaugh et al., "Ultrasound-specific segmentation via decorrelation and statistical region-based active contours," in *CVPR '06*, 2006, vol. 1, pp. 45–53.
- [16] K. Krissian et al., "Speckle-constrained anisotropic diffusion for ultrasound images," in *CVPR '05*, 2005, pp. 547–552.
- [17] Coupé et al., "Fast Non Local Means Denoising for 3D MR Images," in *MICCAI'06*, 2006, LNCS 4191, pp. 33–40.
- [18] M. S. Jensen et al., "A method to obtain reference images for evaluation of ultrasonic tissue characterization techniques," *Ultrasonics*, vol. 40, no. 1-8, pp. 89–94, 2002.